Available online at www.sciencedirect.com

SCIENCE DIRECT

Virology 339 (2005) 81 – 100

VIROLOGY

www.elsevier.com/locate/yviro

Complete genome sequence analysis of an iridovirus isolated from the orange-spotted grouper, *Epinephelus coioides*

Ling Lü[a,1], Song Y. Zhou[a,1], Cheng Chen[a], Shao P. Weng[a,b], Siu-Ming Chan[b], Jian G. He[a,*]

[a]*State Key Laboratory for Biocontrol, School of Life Sciences, Zhongshan University, Guangzhou 510275, P. R. China*
[b]*Department of Zoology, The University of Hong Kong, Hong Kong, P. R. China*

Received 25 February 2005; returned to author for revision 9 March 2005; accepted 11 May 2005
Available online 20 June 2005

Abstract

Orange-spotted grouper iridovirus (OSGIV) was the causative agent of serious systemic diseases with high mortality in the cultured orange-spotted grouper, *Epinephelus coioides.* Here we report the complete genome sequence of OSGIV. The OSGIV genome consists of 112,636 bp with a G + C content of 54%. 121 putative open reading frames (ORF) were identified with coding capacities for polypeptides varying from 40 to 1168 amino acids. The majority of OSGIV shared homologies to other iridovirus genes. Phylogenetic analysis of the major capsid protein, ATPase, cytosine DNA methyl transferase and DNA polymerase indicated that OSGIV was closely related to infectious spleen and kidney necrosis virus (ISKNV) and rock bream iridovirus (RBIV), but differed from lymphocytisvirus and ranavirus. The determination of the genome of OSGIV will facilitate a better understanding of the molecular mechanism underlying the pathogenesis of the OSGIV and may provide useful information to develop diagnosis method and strategies to control outbreak of OSGIV.

Keywords: OSGIV; Iridoviruses; Genome; Sequence analysis

Introduction

Iridoviruses are icosahedral cytoplasmic DNA virus that can infect invertebrates and poikilothermic vertebrates including the insects, fishes, amphibians, and reptiles (Williams, 1996). The viral genomes are both circularly permuted and terminally redundant which is a unique feature among eukaryotic virus genomes (Darai et al., 1983, 1985; Delius et al., 1984; Goorha and Murti, 1982). Additionally, the iridoviruses infect vertebrates that have highly methylated genomes (Darai et al., 1983; Tidona and Darai, 1997; Willis and Granoff, 1980). Currently, the entire genomes of nine iridoviruses have been completely sequenced. These viruses include lymphocystis disease virus 1 (LCDV-1, the type species of the genus *Lymphocystivirus*; Tidona and Darai, 1997; accession no. L63545), infectious spleen and kidney necrosis virus (ISKNV; He et al., 2001; accession no. AF371960), *Chilo* iridescent virus (CIV, the type species of the genus *Iridovirus*; Jakob et al., 2001; accession no. AF303741), tiger frog virus (TFV; He et al., 2002; accession no. AF389451), *Ambystoma tigrinum* virus (ATV; Jancovich et al., 2003; accession no. AY150217), lymphocystis disease virus isolated in China (LCDV-C; Zhang et al., 2004; accession no. AY380826), frog virus 3 (FV3, the type species of the genus *Ranavirus*; Tan et al., 2004; accession no. AY548484), Singapore grouper iridovirus (SGIV; Song et al., 2004; accession no. AY521625), and rock bream iridovirus (RBIV; Do et al., 2004; accession no. AY532606). Most of these viruses can infect low vertebrates except CIV, which is isolated from insects.

Based on the Seventh Report of the International Committee on Taxonomy of Virus (ICTV), the family Iridoviridae has been subdivided into four genera, including *Iridovirus*, *Chloriridovirus*, *Ranavirus*, and *Lymphocystisvirus* (van Regenmortel et al., 1999). Another type of iridoviruses from affected fish, which belong to neither lymphocystivirus nor ranavirus, can cause enlargement of cells in many tissues, especially in the spleen and kidney of

* Corresponding author. Fax: +86 20 84036215.
E-mail address: lsbrc05@zsu.edu.cn (J.G. He).
[1] These authors contributed equally to this work.

0042-6822/$ - see front matter © 2005 Elsevier Inc. All rights reserved.
doi:10.1016/j.virol.2005.05.021

fish. He et al. (2001) tentatively referred them as cell hypertrophy iridoviruses. In 2003, Chinchar et al. proposed a new genus, *Megalocystivirus*, to the International Committee on Taxonomy of Virus (ICTV). The proposed classification system of the family Iridoviridae included *Iridovirus*, *Chloriridovirus*, *Ranavirus*, *Lymphocystisvirus*, and *Megalocystivirus* (personal communication).

In recent years, megalocystiviruses have attracted much research attention because of their ecological and economic impact on wild and cultured fishes. Megalocystiviruses are well-known causative agents of many serious systemic diseases occurred in economically important freshwater and marine fish worldwide. Fishes infected by the megalocystivirus include the red sea bream, *Pagrus major* (Inouye et al., 1992); sea bass, *Lateolabrax* sp. (Nakajima and Sorimachi, 1995); brown-spot grouper, *Epinephelus tauvina* (Chua et al., 1994); Malabar grouper, *E. malabaricus* (Danayadol et al., 1996); angelfish, *Pterophyllum scalare* (Rodge et al., 1997); grouper, *Epinephelus* sp. (Chou et al., 1998); tilapia, *Oreochromis niloticus* (McGrogan et al., 1998); mandarin fish, *Siniperca chuatsi* (He et al., 2000); African lampeye, *Aplocheilichthys normani* (Sudthongkong et al., 2001); dwarf gourami, *Colisa lalia* (Sudthongkong et al., 2002); red drum, *Sciaenop socellata* (Weng et al., 2002); rock bream, *Oplegnathus fasciatus* (Jung and Oh, 2000); large yellow croaker, *Larimichthys crocea* (Chen et al., 2003); and turbot, *Scophthalmus maximus* (Shi et al., 2004).

With the rapid development of grouper culture, outbreaks of viral diseases occurred frequently in cultured orange-spotted grouper (*Epinephelus coioides*) in the culture farms of Guangdong Province, China. The causative agent was confirmed to be an iridovirus named orange-spotted grouper iridovirus (OSGIV). OSGIV is closely related to ISKNV, RBIV, and red sea bream iridovirus (RSIV) based on morphology, histopathology, epidemiology, and some nucleotide sequences information. As the disease was important to the orange-spotted grouper cultures, we have performed sequence analysis and molecular characterization of the OSGIV complete genome. We also performed phylogenetic analysis of the OSGIV proteins with that of other iridoviruses and discussed the taxonomic position of OSGIV.

Results and discussion

Determination of the viral genomic DNA sequence

Because no reliable cell lines could be used for the propagation and isolation of OSGIV, PCR was performed using primers of ISKNV to detect/identify diseased grouper. Sequencing of the PCR products revealed that the major capsid protein (MCP), ribonucleotide reductase small chain (RNRS), and cytosine DNA methyl transferase (DMet) of OSGIV shared 95%, 94%, and 95% identities to those of ISKNV at the nucleotide level (data not shown). We then developed a PCR approach to amplify OSGIV genome with the primers from nucleotide sequence of ISKNV (AF371960). The amplified PCR products were about 1000–1200 bp in length. Moreover, large numbers of overlapping primer pairs were designed to fill gaps and to confirm the sequence. The PCR products were purified and the DNA sequences were determined by a PCR sequencing kit (Applied Biosystems, Inc.). With this procedure, about 6× coverage of OSGIV genome sequence was accomplished.

The OSGIV genome contained a double-stranded DNA consisting of 112,636 bp with a G + C content of 54%. Among the sequenced iridoviruses, the size of the OSGIV genome was similar to that of ISKNV (111,362 bp) (He et al., 2001), RBIV (112,080 bp) (Do et al., 2004), FV3 (105,903 bp) (Tan et al., 2004), TFV (105,057 bp) (He et al., 2002), ATV (106,332 bp) (Jancovich et al., 2003), and LCDV-1 (102,653 bp) (Tidona and Darai, 1997), and slightly smaller than that of SGIV (140,131 bp) (Song et al., 2004) and LCDV-C (186,250 bp) (Zhang et al., 2004), but a much smaller than that of the invertebrate iridovirus, CIV (212,482 bp) (Jakob et al., 2001). The G + C content of the OSGIV genome was similar to those of ISKNV (54.8%), RBIV (53%), FV3 (55%), TFV (55%), ATV (54%), and SGIV (48.64%), but much higher than that of LCDV-1 (29.1%), LCDV-C (27.25%), and CIV (28.6%) (Table 1).

The OSGIV genome also contained numerous short direct, inverted, and palindromic repetitive sequences. A highly direct repetitive region was identified at position 24187 to 24642 bp in the OSGIV genome, which was also

Table 1
Summary of genomic information for 10 sequenced iridoviruses

Virus	Genus	Genome size (bp)	G + C content (%)	No. of ORFs	ORF size (aa)	Year determined	Accession no.
OSGIV	Unassigned	112636	54	121	40–1168	2004	AY894343
RBIV	Unassigned	112080	53	118	50–1253	2004	AY532606
ISKNV	Unassigned	111362	54.8	124	40–1208	2001	AF371960
FV3	*Ranavirus*	105903	55	98	50–1293	2004	AY548484
TFV	*Ranavirus*	105057	55	106	40–1294	2002	AF389451
ATV	*Ranavirus*	106332	54	96	32–1294	2003	AY150217
SGIV	*Ranavirus*	140131	48.64	162	41–1268	2004	AY521625
LCDV-1	*Lymphocystivirus*	102653	29.1	195	40–1199	1997	L63545
LCDV-C	*Lymphocystivirus*	186247	27.25	240	40–1193	2004	AY380826
CIV	*Iridovirus*	212482	28.6	468	40–2432	2001	AF303741

found in ISKNV (He et al., 2001). In this region, there are 14 copies of a 12-bp repetitive sequence. The biological function of these repetitive sequences remained unknown.

Coding capacity of the OSGIV genome

Prediction of potential ORFs by the DS GENE 1.5 viral gene prediction program (Accelrys Inc.) and NCBI ORF finder (http://www.ncbi.nlm.nih.gov/gorf/gorf.html). About 121 presumptive ORFs were identified encoding polypeptides ranging from 40 to 1168 amino acid residues (Table 2, Fig. 1). In 121 ORFs, 16 were also found in other iridoviral genomes (Table 2, italic), and 13 of the 16 ORFs had been assigned similarity or putative function based on homologies with other viral or cellular genes. The relative positions of the putative ORFs in the genome were shown in Fig. 1.

The 121 predicted ORFs accounted for 91% of the genetic information in the OSGIV genome, and these ORFs were present on both strands (42% forward, 58% reverse) (Fig. 1). OSGIV had a relatively compact arrangement of ORFs. The average distance in 106 non-overlapping ORFs was about 96 bp with a smallest distance of 2 bp and a maximum distance of 676 bp. Moreover, 33 putative conserved domains or signatures were identified in the NCBI CD-Search database (Table 2).

There are 15 pairs of overlapping ORFs in the OSGIV genome. Of these 15 pairs of ORFs, 12 pairs had an overlapping of 1–7 bp. This is similar to ISKNV (ORF 39R and 40L, 45L and 46L, 80L and 81R, 86L and 87R; He et al., 2001), RBIV (45L and 46L, 57L and 58L; Do et al., 2004), ATV (ORF 6R and 6bR, 43R and 43bR, 61R and 61bR, etc.; Jancovich et al., 2003), and SGIV (ORF 1L and 2R, 7L and 8L, 12L and 13R, etc.; Song et al., 2004). However, 2 pairs of OSGIV ORFs (ORF 11L and 12L, 87R and 88R) were a fragmented form of ISKNV ORFs (10L and 88R) and RBIV ORFs (11L and 84R), respectively.

OSGIV resembles two other megalocystiviruses (i.e., ISKNV and RBIV) in overall genome structure, and the average identity of the homologous ORFs was 97% to RBIV and 90% to ISKNV at the amino acid level. Moreover, 28 homologous genes were completely matched in size and orientation with the OSGIV, RBIV, and ISKNV (Table 2, marked with a superscript g).

Sequence similarities to proteins in databases

The deduced gene products of the 121 ORFs were compared to amino acid sequence in NCBI BLAST program (http://www.ncbi.nlm.nih.gov/BLAST/). Thirty-nine ORFs showed significant homology to functionally characterized proteins from other species. These proteins included structural proteins and enzymes involved in virus replication, transcription, protein modification, and virus–host interaction (Table 2).

DNA replication and repair

Some OSGIV ORFs encoded putative gene products involved DNA replication, modification, and processing, such as DNA polymerase (ORF 22R), DNA repair protein RAD2 (ORF 30L), cytosine DNA methyl transferase (ORF 48L), SNF2 family helicase (ORF 63L), putative replication factor (ORF 60L), and D5 family NTPase (ORF 106L). These ORFs showed 95–100% identity to those of ISKNV, RBIV, or RSIV.

OSGIV ORF 48L encoded a homologue of cytosine DNA methyl transferase. High levels of methylation of cytosine at CpG residues were identified in iridoviruses from vertebrate hosts, such as FV3 (Willis and Granoff, 1980), LCDV-1 (Wanger et al., 1985), EHNV (Eaton et al., 1991), ISKNV (Deng et al., 2001), and TFV (Lü et al., 2001). Methylation was important in the packaging of DNA into virions (Essani, 1990). There was evidence that FV3 DNA methylase can methylate a broad range of natural and synthetic DNAs in vitro (Willis et al., 1984), and have endonuclease activity (Essani, 1990). When the FV3 DNA methylase was absent, the virus can survive, but they lack viral endonuclease activity (Essani, 1990). In other iridoviruses, the deduced gene products of cytosine DNA methyl transferase existed in the genomes of RBIV, ISKNV, ATV, TFV, LCDV-1, and LCDV-C. The function of OSGIV ORF 48L was unknown. Whether it made viral DNA methylation and appeared an endonuclease activity required further investigation.

The predicted amino acid sequence of OSGIV 106L shared high homology to D5 family NTPase. D5 family NTPase is required for viral DNA replication. It is a nucleic acid independent nucleoside triphosphatase. The vaccinia virus D5 gene encodes a 90-kDa protein that is transiently expressed at early time after infection (Evans et al., 1995). Members of D5 protein family were also found in other iridoviruses. D5 protein of OSGIV D5 is 103 kDa and possesses a characteristic extended type A site of the purine nucleotide-binding motif found in NTP-hydrolyzing enzymes. It might have an NTPase activity and play some role in virus DNA replication or deoxyribonucleotide metabolism.

Transcription and nucleotide metabolism

Proteins involved in DNA transcription were found in the OSGIV genome. They were the two largest subunits of the DNA-dependent RNA polymerase (ORF 31L and 36R), transcription elongation factor SII (ORF 32L), mRNA capping enzyme (ORF 64L), and ribonuclease III (ORF 85R). Most of them showed high amino acid identities (94–99%) to those of ISKNV, RBIV, or RSIV. However, the mRNA capping enzyme of OSGIV shared relatively low identity (76%) to that of RBIV.

The putative OSGIV gene products that were related to nucleotide metabolism comprised of ribonucleotide reduc-

Table 2
Potential open reading frames of the OSGIV genome

ORF	Position	Length (aa)[a]	Conserved domain or signature[b] (CD accession no.)	Predicted structure or function[c]	Homologues to RBIV			Homologues to ISKNV			Homologues to other iridoviruses		
					ORF[d]	Length (aa)	Identity (%)	ORF[e]	Length (aa)	Identity (%)	Species	Identity (%)	Accession no.[f]
1L[g]	134–1270	378	Transmembrane amino acid transporter protein (pfam01490)	Transmembrane amino acid transporter protein	1L	378	99	1L	378	95			
2R	1394–1789	131						2L	216	89			
3R	1849–2064	71			3R	71	100						
4L	2110–2613	167			4L	167	100	3L	185	78			
5L	2632–2808	58			5L	58	100						
6L	2883–3548	221	Catalytic domain of CTD-like phosphatases (smart00577)	Catalytic domain of CTD-like phosphatase	6L	221	100	5L	251	95	LCDV-C 148L	36	YP_073653
											SGIV 61R	35	AAS18076
											LCDV-1 82L	33	NP_078678
											FV3 37R	31	YP_031615
											ATV 64R	29	AAP33244
											CIV 335R	29	NP_149818
7L[g]	3793–5154	453	Iridovirus major capsid protein (pfam04451)	Major capsid protein	7L	453	99	6L	453	98	SBIV	100	AAP74203
											GSDIV	100	AAP37443
											RSIV	99	AAP74204
											ALIV	98	AAP37442
											DGIV	98	AAP37441
											LCDV-C 43L	46	YP_025102
											LCDV-1 147L	46	NP_044812
											TFV 96R	44	NP_572010
											ATV 14L	44	YP_003785
											RRV	44	YP_003785
											EHNV	44	AAO32315
											CIV 274L	44	NP_149737
											FV3 90R	43	YP_031669
											BIV	43	AAO32316
											SGIV 72R	42	YP_164167
8L[g]	5171–6628	485		Myristylated membrane protein	8L	485	99	7L	485	97	RSIV	94	BAC66967
											LCDV-C158R	33	YP_073663
											SGIV 88L	31	AAS18103
											FV3 53R	30	YP_031631
											ATV 51L	30	AAP33230
											LCDV-167L	29	NP_078686
											CIV 118L	28	NP_078665
9R	6699–8246	515			9R	515	99	8R	525	88	RSIV	93	BAC66966
10R[g]	8342–8503	53			10R	53	100	9R	53	92			
11L	8662–8895	77			11L	130	98	10L	130	94	LCDV-1 91R	32	NP_078686
											LCDV-C	28	YP_073651

											145R		
12L	8849–9055	68			11L	130	75	10L	130	72			
13L	9052–9312	86						11L	86	99			
14R[g]	9331–9663	110	RING-finger-containing ubiquitin ligase (COG5540)	RING-finger-containing ubiquitin ligase	12R	110	100	12R	110	96			
15R	9670–11067	465	Serine/threonine protein kinases, catalytic domain (cd00180)	Serine/threonine protein kinases	13R	465	100	13R	461	89	CIV 380R	36	NP_149561
											SGIV150R	34	AAS18165
											LCDV-C 178L	31	YP_073682
											ATV 47L	28	AAP33226
											FV3 57R	27	YP_031636
											LCDV-1 43L	25	NP_078729
16R	11322–12296	324			14R	324	100	14R	319	95			
17R[g]	12302–13093	263			15R	263	100	15R	263	95			
18L[g]	13151–13738	195			16L	195	99	16L	195	90			
19L	13753–14088	111			17L	112	99						
20R	14094–14351	85			18L	79	91						
21L	14431–14607	58			19L	58	100						
22R[g]	14623–17469	948	DNA polymerase type-B family; DNA -directed DNA polymerase (cd00145)	DNA polymerase	20R	948	99	19R	948	97	RSIV	98	BAA28669
											LCDV-C 203L	37	YP_073706
											LCDV-1 135R	35	NP_078724
											SGIV128R	36	YP_164223
											FV3 60R	35	YP_031639
											TFV 63R	35	NP_572000
											ATV 44L	35	YP_003817
											CIV 37L	30	AAD48150
23L	17533–17715	60			21L	60	100	20L	62	87			
24L	17851–17973	40						21L	40	95			
25L	18063–19715	550	Appr-1″-p processing enzyme (smart00506)	Putative phosphatase	22L	536	75	22L	499	64	RSIV	93	AAQ07955
26R	19788–22922	1044	Laminin-type epidermal growth factor-like domain (cd00055)	Laminin-type epidermal growth factor-like protein	23R	805	75	23R	856	64	RSIV	83	AAQ07956
27R[g]	23207–24145	312	Ribonucleotide reductase, R2/beta subunit (RNRR2) (cd01049)	Ribonucleotide reductase small chain	26R	312	99	24R	312	96	RSIV	99	BAA82755
28R	24169–24696	175			27R	127	66						
29L	24693–25013	106						26L	107	87			
30L[g]	25035–25931	298	Xeroderma pigmentosum G N- and I-regions (XPGN, XPGI) (cd00128)	DNA repair protein RAD2	28L	298	99	27L	298	98	RSIV	99	BAA82754
											ATV 10L	33	AAP33187
											FV3 95R	32	YP_031674

(continued on next page)

Table 2 (*continued*)

ORF	Position	Length (aa)[a]	Conserved domain or signature[b] (CD accession no.)	Predicted structure or function[c]	Homologues to RBIV			Homologues to ISKNV			Homologues to other iridoviruses		
					ORF[d]	Length (aa)	Identity (%)	ORF[e]	Length (aa)	Identity (%)	Species	Identity (%)	Accession no.[f]
30L[g]	25035–25931	298	Xeroderma pigmentosum G N- and I-regions (XPGN, XPGI) (cd00128)	DNA repair protein RAD2	28L	298	99	27L	298	98	RSIV	99	BAA82754
											TFV 100R	32	NP_572012
											SGIV 97L	30	AAS18112
											LCDV-1 191R	30	NP_078767
											LCDV-C 169R	28	YP_073674
											CIV 369L	22	NP_149832
31L	25948–29454	1168	RNA polymerase I subunit A N-terminus (smart00663); RNA polymerase II, large subunit (KOG0260)	Largest subunit of the DNA-dependent RNA polymerase	29L	1168	99	28L	1159	96	RSIV	98	BAA82753
											TFV 8R	42	NP_571990
											FV3 8R	39	YP_031586
											ATV 6R	39	AAP33183
											SGIV104L	38	AAS18119
											LCDV-C 191R	37	YP_025105
											LCDV-1 16L	36	NP_078624
32L	29461–29682	73	C2C2 Zinc finger; nucleic-acid-binding motif in transcriptional elongation factor TFIIS and RNA polymerases (smart00440); TFIIS, transcription factor S-II (TFIIS) (pfam01096)	Transcription elongation factor SII				29L	73	94	FV3 81R	41	YP_031660
											TFV 86R	41	NP_572006
											ATV 24L	41	AAP33201
											LCDV-1 171R	36	NP_078754
											CIV 349L	29	NP_149812
											SGIV 85R	27	AAS18100
33R[g]	29973–30215	80			30R	80	99	31R	80	85			
34R	30310–30942	210	Deoxynucleotide kinases (COG1428)	Deoxyribonucleo-side kinase	31R	210	100	32R	203	88	ATV 19L	28	AAP33196
											FV3 85R	27	YP_031664
											LCDV-C 27R	26	YP_073536
											LCDV-1 136R	26	NP_078725
											SGIV 67L	25	AAS18082
											CIV 143R	24	NP_149606
35L	31033–31935	300			32L	313	99	33L	313	90			
36R	32018–35176	1052	RNA polymerase Rpb2, domain 6 (pfam00562)	DNA-directed RNA polymerase II second largest subunit-like protein	33R	1053	98	34R	1044	96	LCDV-C 25R	43	YP_073534
											LCDV-1 25L	43	NP_078633
											SGIV 73L	41	AAS18088
											FV3 62L	40	YP_031641
											TFV 65L	40	NP_572001
											ATV 43R	39	AAP33221

37L	35249–36382	377			34L	377	99	35L	382	88			
38R	36376–37431	351						36R	351	91			
39L	37428–38777	449			37L	369	82	37L	450	91			
40L	38786–40225	479			38L	501	99	38L	478	87			
41R	40290–41168	292						39R	290	89			
42L	41161–42306	381			41L	381	99	40L	379	89			
43L	42308–43657	449			42L	449	99	41L	447	88			
44R	43672–44271	199						42L	197	88			
45L	44355–44717	120	Erv1/Alt family (pfam04777)	Thiol oxidoreductase				43L	120	98	FV3 88R	37	YP_031667
											ATV 16L	37	AAP33193
											SGIV 70R	36	AAS18085
											LCDV-1 81R	33	NP_078699
											LCDV-C 142L	30	YP_073647
46L[g]	44724–45524	266			44L	266	99	44L	266	87			
47L[g]	45529–46443	304			45L	304	99	45L	304	87			
48L[g]	46437–47120	227	Cytosine-C5-specific DNA methylases (cd00315)	Cytosine DNA methyl transferase	46L	227	99	46L	227	96	LCDV-C 86L	57	YP_025103
											ATV 21L	43	YP_003792
											FV3 83R	42	YP_031662
											TFV 89R	42	NP_572009
											LCDV-1 5L	37	NP_078617
49R	47280–47543	87						47R	87	98			
50R	47540–47893	117	Platelet-derived and vascular endothelial growth factors (PDGF, VEGF) family domain (cd00135)	Vascular endothelial growth factor-like protein				48R	114	85			
51R	47909–48079	56						49R	56	89			
52L[g]	48147–48575	142			49L	142	100	50L	142	90			
53L[g]	48854–49306	150			50L	150	99	52L	150	83			
54R	49308–49502	64			51R	64	98	53R	71	81			
55L	49536–50480	314			52L	314	99	54L	308	93			
56L	50503–51444	313			53L	313	100	55L	308	78	LCDV-1 10L	46	NP_078687
											LCDV-C 80R	43	YP_073689
											FV3 19R	25	YP_031597
											ATV 80L	25	AAP33261
											SGIV 39L	25	AAS18054
57L[g]	51455–52102	215			54L	215	99	56L	215	98	LCDV-1 6L	39	NP_078618
												37	
											FV3 21L	37	YP_031599
											ATV 78R	35	AAP33259

(continued on next page)

Table 2 (*continued*)

ORF	Position	Length (aa)[a]	Conserved domain or signature[b] (CD accession no.)	Predicted structure or function[c]	Homologues to RBIV			Homologues to ISKNV			Homologues to other iridoviruses		
					ORF[d]	Length (aa)	Identity (%)	ORF[e]	Length (aa)	Identity (%)	Species	Identity (%)	Accession no.[f]
57L[g]	51455–52102	215			54L	215	99	56L	215	98	LCDV-1 6L	39	NP_078618
											SGIV 54R	32	AAS18069
											LCDV-C 7L	28	YP_073516
											CIV 67R		NP_149530
58L[g]	52109–52369	86			55L	86	100	57L	86	95			
59L	52634–53146	170			56L	170	99						
60L	53210–54016	268		Putative replication factor	57L	268	99	61L	267	96	CIV 282R	32	NP_149745
											LCDV-C 75L	26	YP_073685
											SGIV116R	25	AAS18131
											LCDV-1 162L	24	NP_078747
											FV3 1R	23	YP_031579
											ATV 91R	22	AAP33272
61L	54013–55131	372			58L	1253	99	62L	1208	96			
62L	55163–57862	899			58L	1253	98	62L	1208	84			
63L[g]	58228–60876	882	DEAD-like helicases superfamily (cd00046)	SNF2 family helicase	59L	882	99	63L	882	95	SGIV 60R	33	AAS18075
											FV3 9L	32	YP_031587
											TFV 9L	32	NP_571991
											ATV 7L	32	AAP33184
											LCDV-C 75L	32	YP_073582
											LCDV-1 132L	32	NP_078720
											CIV 22L	26	NP_149485
64L	60944–62416	490	Dual specificity phosphatases (DSP); Ser/Thr and Tyr protein phosphatases (cd00127)	mRNA capping enzyme	60L	415	76	64L	491	96			
65L	62458–62928	156	RING-finger domain (cd00162)	RING-finger-containing E3 ubiquitin ligase	61L	155	98	65L	253	95			
66L	62979–64061	360	RING-finger domain (cd00162)	RING-finger-containing E3 ubiquitin ligase	62L	365	99	66L	347	87			
67L	64213–64446	77			63L	77	100						
68R	64440–64565	41						67R	199	78			
69L[g]	64801–66234	477			64L	477	99	68L	477	94			
70L	66246–66977	243			65L	186	68	69L	221	81			
71L	67417–68973	518			68L	469	90	71L	536	91			
72R	69078–69497	139						73R	139	87			
73R	69546–70568	340			70R	339	99	74R	337	92			

74L	70669–70938	89			71L	89	99	75L	88	94			
75L	70940–73912	990			72L	998	95	76L	990	96	CIV 295L	37	NP_149758
											FV3 41R	25	YP_031619
											ATV 69R	25	AAP33249
											LCDV-C 235R	24	YP_073738
											SGIV 57L	23	AAS18072
											LCDV-1 163R	22	NP_078748
76R	73930–75264	444	Ankyrin repeats (cd00204)	Ankyrin repeat-containing protein				77R	444	92			
77R[g]	75261–75725	154			75R	154	100	78R	154	97			
78L	75727–75951	74			76L	74	100	79L	73	95			
79R	76039–76512	157			77R	157	100						
80R[g]	76525–77022	165			78R	165	99	81R	165	97			
81L[g]	77071–78177	368			79L	368	99	82L	368	95			
82R	78202–78600	132			80R	132	98						
83L	78627–79931	434			81L	434	99	84L	451	86			
84R	80018–80548	176			82R	176	100	85R	200	77			
85R	80978–81775	265	Ribonuclease III family (smart00535); dsRNA-specific ribonuclease (COG0571)	Ribonuclease III	83R	265	98	87R	256	96	SGIV 84L	34	AAS18099
											LCDV-C 187R	31	YP_073691
											LCDV-1 137R	30	NP_078726
											FV3 80L	30	YP_031659
											TFV 85L	30	NP_572005
											ATV 25R	29	AAP33202
											CIV 142R	23	NP_149605
86R	81878–82279	133			84R	640	84	88R	667	82			
87R	82234–83805	523			84R	640	97	88R	667	92			
88L	84000–84134	44						91L	79	90			
89R	84810–84995	61						92R	91	96			
90L[g]	84992–85918	308			86L	308	99	93L	308	94			
91L[g]	85928–86428	166			87L	166	99	94L	166	96			
92L	86453–87616	245			88L	387	99	95L	386	91			
93L	87624–88361	245						96L	270	89	LCDV-C 100L	30	YP_073606
											FV3 12L	29	YP_031590
											ATV 87R	28	AAP33268
											LCDV-1 108L	26	NP_078701
											SGIV118R	24	AAS18133
											CIV 287R	21	NP_149750
94L	88366–88857	163			90L	162	99				LCDV-1 59L	25	NP_078659
											LCDV-C 157R	19	YP_073662

(continued on next page)

Table 2 (*continued*)

ORF	Position	Length (aa)[a]	Conserved domain or signature[b] (CD accession no.)	Predicted structure or function[c]	Homologues to RBIV			Homologues to ISKNV			Homologues to other iridoviruses		
					ORF[d]	Length (aa)	Identity (%)	ORF[e]	Length (aa)	Identity (%)	Species	Identity (%)	Accession no.[f]
95L[g]	88906–89229	107	RING-finger domain (cd00162)	RING-finger domain-containing E3 protein	91L	107	100	99L	107	83			
96L	89377–90024	215			92L	215	99	100L	181	89			
97L	89993–90508	171						101L	171	94			
98R	90577–92022	481	Ankyrin repeats (cd00204)	Ankyrin repeat-containing protein	94R	481	100	102R	480	91			
99R	92029–92442	137	Src homology 2 domains (cd00173)	Suppressor of cytokine signaling protein				103R	133	80			
100R	92501–93280	259			96R	259	99	104R	258	90			
101R	93282–93653	123			97R	123	100	105R	121	97			
102R	93747–94634	295	HINT (histidine triad nucleotide-binding protein) subgroup (cd01277)	HINT protein	98R	295	100						
103L	94676–95548	290			99L	273	99	106L	339	78			
104L	95799–95936	45						107L	71	88			
105R	95992–96276	94			100R	94	85	108R	49	77			
106L	96298–99060	920	Predicted ATPase (COG3378); Poxvirus D5 protein-like (pfam03288)	D5 family NTPase	101L	921	99	109L	921	97	LCDV-C 80L	36	YP_073585
											SGIV 52L	36	AAS18067
											FV3 22R	35	YP_031600
											ATV 77L	35	AAP33258
											LCDV-1 128L	34	NP_078717
											CIV 184R	28	NP_149647
107R	99113–99268	51						110R	51	90			
10 8L	99265–99885	206	Tnf receptor-associated factor 2 domain (cd00270); MATH (cd00121)	Tumor necrosis factor type 2 receptor-associated protein	102L	298	91	111L	296	83			
109R	100183–100926	247		Proliferating cell nuclear antigen	103R	146	98	112R	247	97	LCDV-1 3L	31	NP_078615
											LCDV-C 197L	28	YP_073700
											SGIV 68L	28	AAS18083
											ATV 20L	24	AAP33197
											FV3 84R	23	YP_031663
110R	100998–101414	138						113R	117	96			

111L	101594–104041	815	CAP10, putative lipopolysaccharide-modifying enzyme (smart00672)	Tyrosine kinase	106L	358	95	114L	941	81	FV3 27R	43	YP_031605
											TFV 29R	43	NP_571995
											ATV 58R	43	AAP33237
											SGIV 81L	42	AAS18093
											LCDV-C 173R	24	YP_073677
											CIV 179R	23	NP_149902
											LCDV-1 195R	20	NP_078770
112R	104476–105486	336		Immediate early protein ICP-46	108L	243	89	115R	336	97	LCDV-1 47L	33	NP_078648.1
											LCDV-C 162R	25	YP_073667.1
											TFV 97R	24	NP_572011.1
											FV3 91R	23	YP_031670.1
											ATV 13L	22	AAP33190.1
											SGIV162L	20	AAS18177.1
											CIV 393L	20	NP_149856.1
113R	105547–106701	384			110R	477	95	116R	482	86			
114L[g]	106978–107652	224		Early 31 kDa protein	111L	224	99	117L	224	95	FV3 23R	24	YP_031603
											TFV 25R	24	NP_571993
											LCDV-C 34L	24	YP_025101
											LCDV-1 122R	23	NP_078713
											ATV 55R	23	AAP33234
											SGIV 6R	22	AAS18021
115L	107986–109299	437	Ankyrin repeats (cd00204)	Ankyrin repeat-containing protein	112L	454	98	118L	456	93			
116R	109369–109656	95	RING-finger domain (cd00162)	RING-finger domain-containing E3 protein	113R	57	98	119R	95	95			
117R	109687–110193	168			114R	129	84	120R	169	93			
118L	110214–110849	211			115L	149	88	121L	216	65			
119R[g]	110859–111578	239		ATPase	116R	239	100	122R	239	98	RSIV	100	BAA28670
											SBIV	100	BAA96406
											LBIV	100	AAL68654
											TGIV	100	BAA96407
											GSIV	100	AAL68653
											LYCIV	99	AAO16492
											ALIV	99	BAA96408
											DGIV	99	AAP74205
											GIV	54	AAL68652
											LCDV-C 114L	54	YP_073620
											LCDV-1 54R	53	NP_078656

(continued on next page)

Table 2 (*continued*)

ORF	Position	Length (aa)[a]	Conserved domain or signature[b] (CD accession no.)	Predicted structure or function[c]	Homologues to RBIV			Homologues to ISKNV			Homologues to other iridoviruses		
					ORF[d]	Length (aa)	Identity (%)	ORF[e]	Length (aa)	Identity (%)	Species	Identity (%)	Accession no.[f]
119R[g]	110859–111578	239		ATPase	116R	239	100	122R	239	98	RSIV	100	BAA28670
											SGIV134L	51	YP_164229
											FV3 16R	51	YP_031593
											ATV 83L	50	YP_003858
											TFV 16R	50	NP_571992
											CIV 75L	38	NP_149538
120R	111656–111850	64			117R	64	98	123R	61	93			
121L	111939–112625	228	Ankyrin repeats (cd00204)	Ankyrin repeat-containing protein	118L	153	90	124L	228	95			

Note. italicized data denote common ORFs among RBIV, ISKNV, FV3, ATV, TFV, SGIV, LCDV-1, LCDV-C, and CIV.

[a] aa—number of amino acids of each OSGIV putative protein.

[b] Conserved domain or signature was constructed using the program CD-Search within BlastP.

[c] Function was deduced from the degree of amino acid similarity to products of known genes.

[d] Best matched ORF from the RBIV genome.

[e] Best matched ORF from the ISKNV genome.

[f] Accession numbers were derived from the NCBI database.

[g] Completely matched ORFs in same size and orientation among OSGIV, RBIV, and ISKNV.

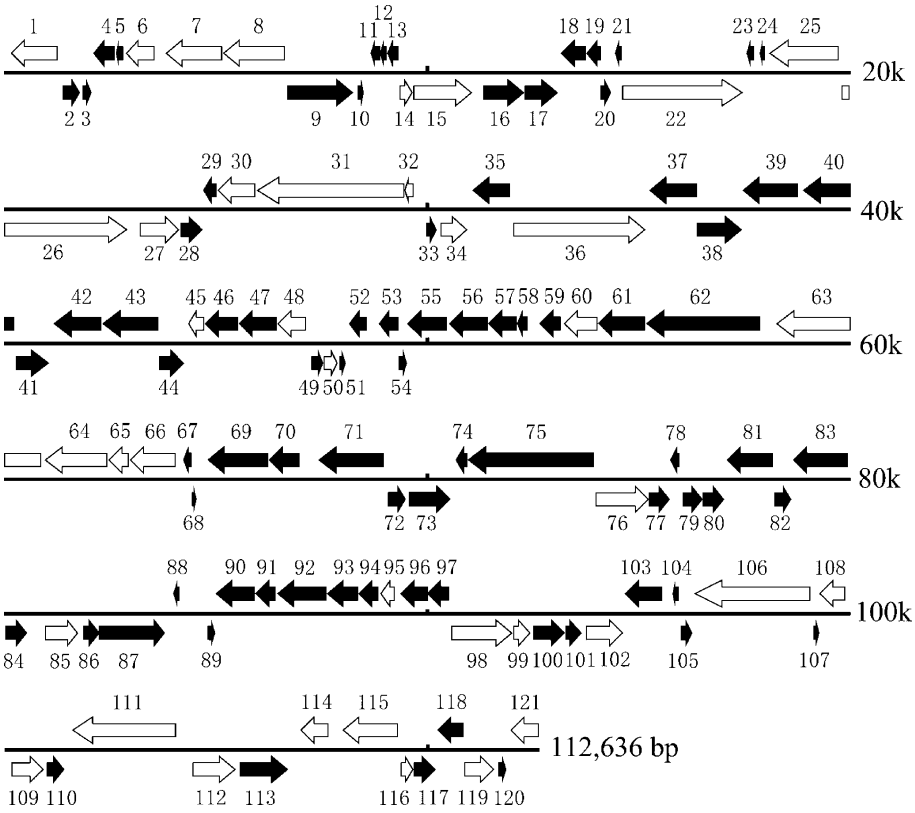

Fig. 1. Organization of the OSGIV genome. Arrows that indicated the location, orientation, and putative size represent each ORF. White arrows represent ORFs with predicted function to other organisms, and black arrows represent ORFs with unknown function.

tase small subunit (ORF 27R) and deoxyribonucleoside kinase (ORF 34R). DNA is made of four deoxyribonucleoside triphosphates, provided by the de novo and salvage pathways. The key enzyme of the de novo pathway is ribonucleotide reductase. ORF 27R of OSGIV encoded a ribonucleotide reductase small subunit, which may catalyze a rate-limiting reaction in which ribonucleoside diphosphates are converted to their corresponding deoxyribonucleoside diphosphates. The precursors of deoxyribonucleoside triphosphates (dNTPs) are required for DNA synthesis and repair (Lammers and Follmann, 1983). ORF 34R encoded a homologue of deoxyribonucleoside kinase, the key enzymes of salvage pathways, which phosphorylate deoxyribonucleosides to the corresponding deoxyribonucleoside monophosphates (Arnér and Eriksson, 1995; Lammers and Follmann, 1983).

Protein modification

OSGIV contained three genes with putative protein modification function. These genes included a serine/threonine protein kinase (ORF 15R), a thiol oxidoreductase (ORF 45L), and a tyrosine kinase (ORF 111L).

ORF 45L encoded a thiol oxidoreductase with Erv1/Alr domain (Erv1, essential for respiration and vegetative growth; Alr, augmenter of liver regeneration). The Erv1/Alr family is a large family encoded by cytoplasmic DNA viruses and all eukaryotes (Senkevich et al., 2000). It includes the *Saccharomyces cerevisiae* Erv1 protein, which is required for mitochondrial biogenesis, and it's the mammalian homologues hematopoietin (named ALR). Both Erv1p and full-length ALR are located in the mitochondrial intermembrane. The conserved domain of the ERV1/ALR protein consists of about 100 amino acid residues and contains an invariant thiol active-site motif C-X-X-C (Senkevich et al., 2000). The functions of many ERV1/ALR proteins remain unknown, but they may represent a ubiquitous class of cellular thiol oxidoreductases. The C-X-X-C motif of the ERV1 domain is the redox-active disulfide bridge of secreted egg-white sulfhydryl oxidase, a member of the quiescin family (Senkevich et al., 1997). The deduced OSGIV Erv1/Alr protein consisted of 120 amino acid residues, and it contained a thiol active-site motif C-K-T-C, which suggested that it might participate in thiol-disulfide metabolism and protein folding.

Host-related function

OSGIV contained a significant number of putative genes that exhibit similarity to cellular genes and other iridovirus genes. There were five ORFs predicted to encode RING finger proteins (RFPs) (ORF 14R, 65L, 66L, 95L, and 116R). They were highly homologous to those of ISKNV (ORF 12R, 65L, 66L, 99L, and 119R). The study on Ring

finger protein showed that the four RFPs of ISKNV (ORF 12R, 65L, 66L, and 111L) acted as the E3 enzyme in the presence of ubiquitin activating enzyme (E1), ubiquitin, zincion, and specific E2 (UbcH5 subfamily). The RING domain of RFP in ISKNV (ORF 66L) was proved to be essential for the activity of E3 enzyme by the mutational analysis (unpublished data). The functions of the RFPs in OSGIV remained unknown, but these RFPs in OSGIV may have E3 activity considering their high homology (83–96% amino acids identities) to those in ISKNV (Table 2).

ORF 99R of OSGIV encoded a Src homology 2 (SH2) domain-containing protein. SH2 domain is involved in recognition of phosphorylated tyrosine (pTyr). It binds to pTyr-containing ligands via two surface pockets, a pTyr and a hydrophobic-binding pocket, allowing proteins with SH2 domains to localize to tyrosine-phosphorylated sites. Some SH2 domain-containing proteins (such as SLP-76, Shb, and SHIP) play a role in phosphoinositide 3-kinase (PI3K) signaling pathways (Shim et al., 2004; Lu et al., 2002; Rauh et al., 2003). ORF 50R encoded a protein that contained vascular endothelial growth factor (VEGF) family domain. Recent studies showed that VEGF could stimulate the PI3K signaling pathways and inhibit apoptosis in the viral-infected host cells (Brader and Eccles, 2004; Gelinas et al., 2002; Takahashi et al., 2003). Further investigation is needed to determine whether both ORF 50R and ORF 99R participate in the PI3K signaling pathways in the viral-infected host cells.

In addition, some important putative genes involved in host-related function were found in the OSGIV genome, such as ankyrin repeat motifs (ORF 76R, 98R, 115L, and 121L), the C-terminal domain (CTD)-like phosphatase (ORF 6L), proliferating cell nuclear antigen (ORF 10R), laminin-type epidermal growth factor (EGF)-like domain (ORF 26R), and tumor necrosis factor receptor-associated factor (TRAF, ORF 108L).

Putative membrane-associated proteins

The ORFs of OSGIV were analyzed for the presence of putative transmembrane domains (TMs). One or more putative TMs (1–11) were found in 5 ORFs (ORF 1L, 5L, 52L, 53L, and 94L) with the computer software TMHMM 2.0 (Krogh et al., 2001). These proteins contain a putative TM probably associated with membrane structures. These hydrophobic domains may be involved in protein–protein interactions that are necessary for the formation of the nucleocapsid globular subunits (van Hulten et al., 2001).

Other proteins

OSGIV also encoded proteins homologous to a phosphatase (ORF 113R), an ATPase (ORF 119R), a protein containing HINT (histidine triad nucleotide-binding protein) domain (ORF 102R), and a structural protein (major capsid protein, ORF 7L).

ORF 102R encoded a protein containing a HINT domain. HINT belongs to a superfamily of histidine triad (HIT) hydroxylases that act on alpha-phosphate of ribonucleotides. HINT consists of small homodimerizing proteins characterized by conserved histidine residues His-X-His-X-His-X-X (X, a hydrophobic amino acid) near their C-terminal ends (Brenner, 2002). HINT is the most widely conserved feature of the HIT superfamily, and HINT homologues are present in a wide variety of organisms in the metazoan, plant, fungus, bacterium, and virus. Although the biochemical function has not been characterized for many of the members of HINT, the proteins from yeast have been shown to be involved in secretion, peroxisome formation, and gene expression (Bieganowski et al., 2002). The deduced product of OSGIV ORF 102R was 295 amino acids in length with a “H-A-H-A” region near its C-terminal end, and it may be involved in gene expression in the viral-infected host cells.

Relationship of OSGIV to ISNNV and RBIV

The comparative analysis of the OSGIV, RBIV, and ISKNV revealed many homologues (Table 2). Many ORFs of the three-iridoviral genomes including the conserved genes and other ORFs of unknown function were similar in size, structure, and composition. 98 and 109 ORFs of OSGIV had homologies to that of RBIV (66–100%) and ISKNV (64–99%) at the amino acid level, respectively (Do et al., 2004; He et al., 2001). Comparing OSGIV and RBIV, 98 ORFs of OSGIV had homologies (average 97%) to those of RBIV; 63 of the 98 ORFs had same size and the identities varied from 85% to 100%; 35 of the 98 ORFs were differed in size with identities varied from 66% to 99%. Comparing OSGIV with ISKNV, 109 ORFs showed homologies to those of ISKNV with average identity of 90%; 43 of 109 ORFs had the same size and the identities vary from 83% to 99%; 66 of 109 ORFs had different sizes and their identities vary from 64% to 96%.

DNA dot matrix analyses of OSGIV genomic DNA with itself (Fig. 2A), the ISKNV genome (Fig. 2B) and the RBIV genome (Fig. 2C) were performed using DS GENE 1.5 (Accelrys Inc.). The results revealed that the gene order between OSGIV and ISKNV, OSGIV, and RBIV was markedly conserved. The arrowhead at Fig. 2A showed repeat sequences indicated by the short parallel lines offset from the consensus diagonal. A highly direct repetitive region (24187–24642 bp) was identified from Fig. 2A, which was consistent with the result using the GeneQuest program (Lasergene). Despite the high sequence similarity among OSGIV, ISKNV, and RBIV, Fig. 2B showed several insertions or deletions between OSGIV and ISKNV indicated by gaps in the consensus line, and they were mainly in the OSGIV genome nucleotides position 18500–23500, 54000–62000, 69000–69500, 75800–76600, and 93500–94750 bp. The insertions or deletions were also observed between OSGIV and RBIV (Fig. 2C), and they

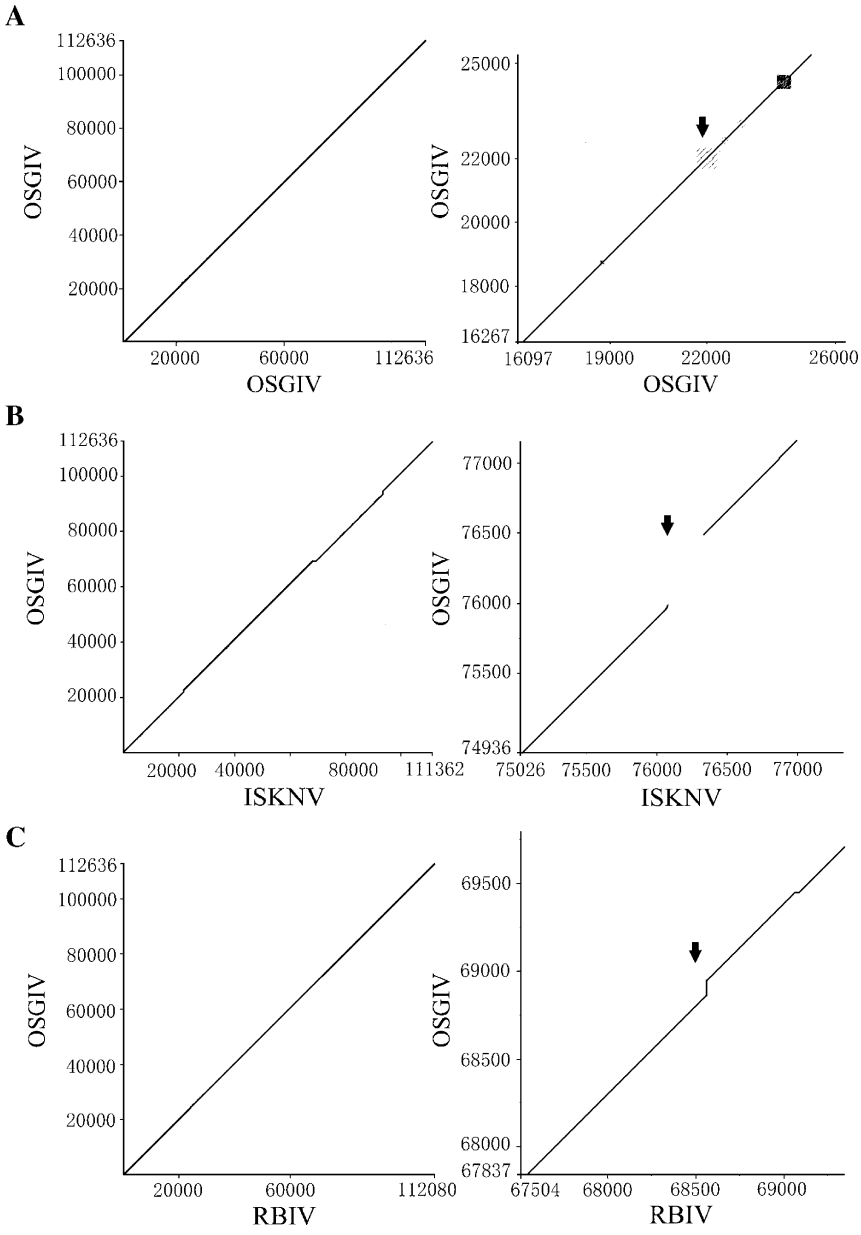

Fig. 2. Dot matrix plots comparing the OSGIV genome (vertical axis) with the ISKNV, RBIV genome, and itself (horizontal axis). The horizontal axes represent (A) the OSGIV genome; (B) the ISKNV genome; (C) the RBIV genome. The complete genomic sequences were aligned using DS GENE 1.5. The arrowheads indicate repeat sequences (A), insertions, or deletions (B and C).

were mainly located in the OSGIV genome nucleotides position 21500–23000, 52000–57000, 67000–69000, 82000–85000, and 105100–107700 bp. But when compared Fig. 2B with Fig. 2C, the gaps of Fig. 2C were less than those of Fig. 2B, which suggested that OSGIV was more colinear to RBIV than to ISKNV.

The similarity among OSGIV, RBIV, and ISKNV indicated a close structural and functional relationship. Additionally, the differences in the size and homology among ORFs of three viruses may result in the differences in the natural hosts and mortality. For example, in a recent study, we have shown that OSGIV could infect the fresh water mandarin fish that is the natural host of ISKNV. The mortality of mandarin fish infected by OSGIV was about 40% (unpublished data), but it could reach 100% if it was infected by ISKNV (He et al., 2000).

Relationship of OSGIV to other iridoviruses

Iridoviral sequences available in data banks were compared to the complete sequence of OSGIV, and the result showed that the putative gene products of OSGIV shared high homology to the corresponding viral proteins of other iridoviruses (Table 2). There were some homologous genes in the OSGIV, ISKNV, RBIV, TFV, FV3, ATV, SGIV, LCDV-1, and LCDV-C genomes. These included genes for the DNA

polymerase (DdDP), the DNA methyl transferase (DMet), the SNF2-like helicase, the XPG/RAD2-type nuclease (RAD2), the two large subunit of DNA-dependent RNA polymerase (DdRPI and DdRPII), the RNase III (RIII), the ATPase and the major capsid protein (MCP) involved in virus replication, transcription, modification, and structural composition. Fig. 3 showed the comparison of OSGIV with other eight vertebrate iridoviruses. Since the origin of replication was unknown, the start codon (ATG) of MCPs gene was chosen as the first base for all viral genomes. However, as MCP of OSGIV, RBIV, ISKNV, ATV, LCDV-1, and LCDV-C were present on antisense strands of the genomes, we shifted sense and antisense strands on these viruses in order to get the same nucleotide order on MCPs individually. It was obvious that these homologous genes of OSGIV, RBIV, and ISKNV were located at similar map position and colinearity was detected in the three virus genomes. In contrast, these gene orders on the OSGIV genome were significant different with those of ranaviruses and lymphocystiviruses. This figure indicated that OSGIV was more closely related to RBIV and ISKNV, and markedly differed from members of the genus *Ranavirus* and *Lymphocystivirus*.

Phylogenetic analysis

In order to determine the phylogenetic relationship of OSGIV to other iridoviruses, the amino acid sequence of the major capsid protein (MCP) was used in an alignment with other iridoviruses from GenBank. MCP is a suitable target for the phylogenetic studies as it is highly conserved in iridoviruses (Tidona et al., 1998; Hyatt et al., 2000). The amino acid sequence of MCP share > 98% identity with OSGIV, RBIV, and ISKNV, respectively, but it shared low identity (< 47%) to that of ranaviruses and lymphocystiviruses. It is the predominant structural component of the virus particles comprising 40–50% of the total particle polypeptide (Williams, 1996). The neighbor-joining tree (Saitou and Nei, 1987) of MCP was constructed and it assigned the iridoviruses to four groups: group I, ranaviruses, including FV3, TFV, ATV, RRV, BIV, EHNV, and SGIV; group II, lymphocystiviruses, including LCDV-1 and LCDV-C; group III, megalocystiviruses, including OSGIV, ISKNV, RBIV, RSIV, SBIV, GSDIV, ALIV, and DGIV; group IV, the insect iridoviruses, including CIV, CzIV, SIV, TIV, and WIV; PBCV-1 was used as an outgroup (Fig. 4A). The results illuminated that OSGIV was more closely related to RBIV, ISKNV, RSIV, SBIV, GSDIV, ALIV, and DGIV as compared to the *Ranavirus* and *Lymphocystiviruses*. Additionally, the highly conserved full-length protein sequences of the ATPase, cytosine DNA methyl transferase, and DNA polymerase from the iridoviruses were used for phylogenetic analysis (Figs. 4B–D). These trees also supported the view that OSGIV was more closely related to RBIV and ISKNV.

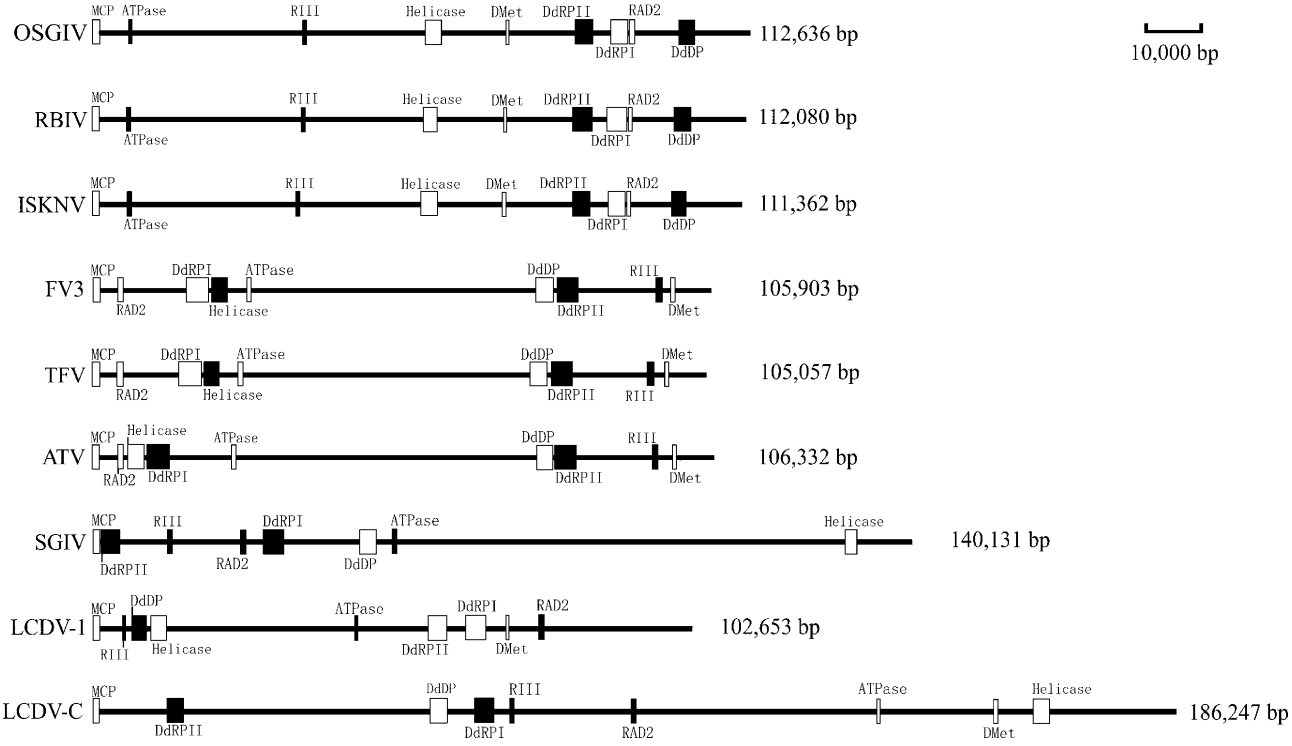

Fig. 3. Organization comparison of some conserved genes of the OSGIV, RBIV, ISKNV, FV3, TFV, ATV, SGIV, LCDV-1, and LCDV-C genomes. The line indicates the genome of the corresponding iridovirus, and the squares indicate the approximate size of the conserved genes including the DNA polymerase (DdDP), the DNA methyl transferase (DMet), the SNF2-like helicase (Helicase), the XPG/RAD2-type nuclease (RAD2), the two largest subunit of DNA-dependent RNA polymerase (DdRPI and DdRPII), the RNase III (RIII), the ATPase, and the major capsid protein (MCP). The direction of transcription forward is represented by an open square, and solid squares correspond to the reverse direction.

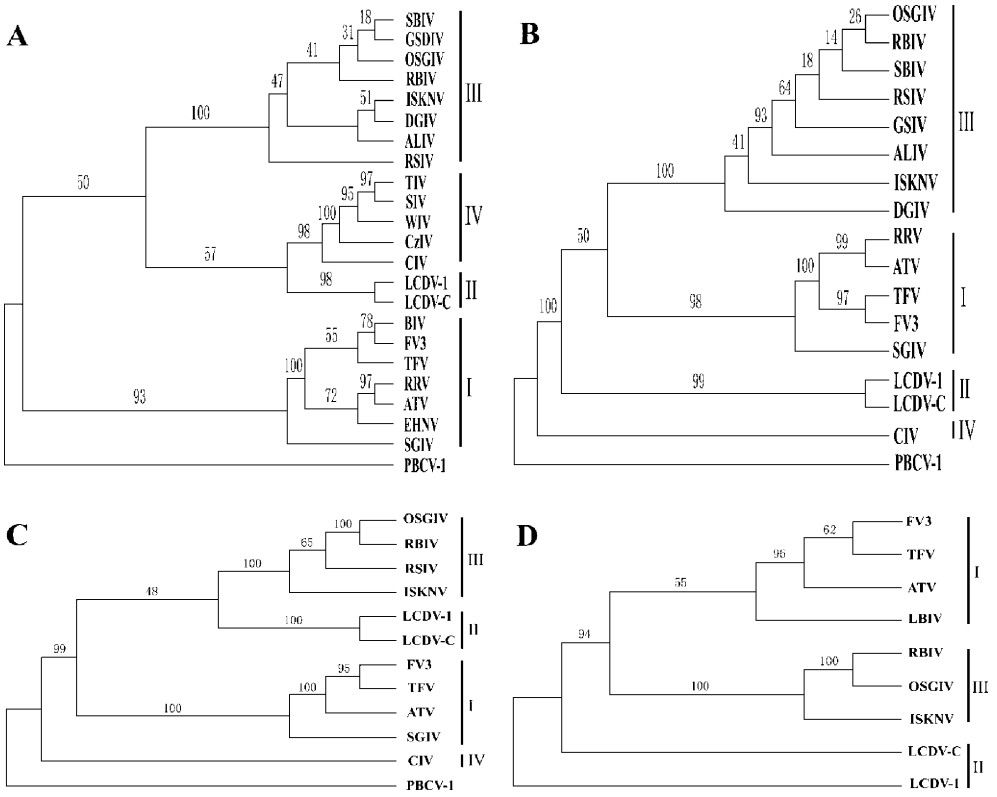

Fig. 4. Phylogenetic relationships of iridovirus obtained using 4 protein sequence alignments: (A) major capsid protein, (B) ATPase, (C) DNA polymerase, (D) cytosine DNA methyl transferase. The alignments were carried out by Clustal X 1.80 and the neighbor-joining trees obtained using PHYLIP 3.6 were shown with the statistical support indicating the robustness of the inferred branching pattern as assessed using the bootstrap test. Accession numbers: (A) ATV, YP_003785; ALIV, AAP37442; BIV, AAO32316; CIV, NP_149737; CzIV, AAB82569; DGIV, AAP37441; EHNV, AA032315; FV3, YP_031669; GSDIV, AAP37443; ISKNV, AAL98730; LCDV-1, NP_044812; LCDV-C, YP_025102; PBCV-1, AAC96798; RBIV, AAS44553; RRV, YP_003785; RSIV, AAP74204; SBIV, AAP74203; SGIV, YP_164167; SIV, AAA66585; TIV, AAA46245; TFV, NP_572010; WIV, AAB82568. (B) ALIV, BAA96408; ATV, YP_003858; CIV, NP_149538; DGIV, AAP74205; FV3, YP_031593; GSIV, AAL68653; ISKNV, AAL98847; LCDV-1, NP_078656; LCDV-C, YP_073620; PBCV-1, AAC96760; RRV, YP_003858; RSIV, BAA28670; SBIV, BAA96406; SGIV, YP_164229; TFV, NP_571992. (C) ATV, YP_003817; CIV, AAD48150; FV3, YP_031639; ISKNV, AAL98743; LCDV-1, NP_078724; LCDV-C, YP_073706; RBIV, AAT71835; RSIV, BAA28669; SGIV, YP_164223; TFV, NP_572000; PBCV-1, NP_048532. (D) ATV, YP_003792; FV3, YP_031662; ISKNV, AAL98770; LBIV, AAC79864; LCDV-1, NP_078617; LCDV-C, YP_025103; RBIV, AAT71861; TFV, NP_572009.

During the past years, a growing number of megalocystiviruses have been isolated from different fish species as the causative agents of diseases due to the significant economic losses of the diseases. These megalocystiviruses included RSIV (Inouye et al., 1992), GIV (Chua et al., 1994), SBIV (Nakajima and Sorimachi, 1995), ISKNV (He et al., 2000), RBIV (Jung and Oh, 2000), DGIV and ALIV (Sudthongkong et al., 2001), LYCIV (Chen et al., 2003), and OSGIV. The phylogenetic analysis strongly suggested that they were not closely related to any of the previously characterized genus of the family Iridoviridae and supported the current taxonomic view that *Ranavirus*, *Lymphocystisvirus*, and *Megalocystivirus* comprised three distinct genera within the family Iridoviridae (personal communication). There were many homologous genes among OSGIV, RBIV, and ISKNV. Most of these genes showed high identities at the amino acid level, but a few of them showed relatively low identities. Meanwhile, some genes shared no identity among the three iridoviruses. The mortality of OSGIV on fish was different from that of ISKNV. For example, the mortality of mandarin fish (the natural host of ISKNV) infected by OSGIV was about 40%, but it could be 100% if affected by ISKNV (unpublished data). For these reasons, we tend to assign OSGIV as a new species of megalocystivirus different from RBIV and ISKNV. However, because of the limited information on its biological characteristics, host range, and geological distribution, more studies are needed to confirm this.

In summary, we have obtained the complete genomic sequence of OSGIV. Most OSGIV genes shared homology with the counterpart of other iridoviruses. From the homologous genes arrangement in the viral genomes, OSGIV, RBIV, and ISKNV were shown to be arranged in a colinear manner. Although the three viruses were similar, some of their genes displayed low identity at the amino acid level. The difference of the genes among the three viruses maybe results in the host specificity. The detailed viral genome analysis will provide valuable information to serve as the genetic basis for future studies and to control the pathogens of the disease.

Materials and methods

Fish

Diseased orange-spotted grouper were obtained from the aquatic farms in Huidong, Guangdong Province, China, in September 2002 when the outbreak of the disease occurred. The diseased fish showed some signs including reduced feeding activity, lethargy, and a darkened body with atypical swimming behavior at the edge of cages in moribund fish. These fish had enlarged spleen and kidney cells checked by histopathology. The spleens and kidneys were removed from diseased fish and the viruses were observed by light and electron microscopy. Meanwhile, some samples were stored at −80 °C, then were examined by PCR to further confirm the disease.

Virus and viral DNA

Spleen and kidney from the diseased fish were rinsed 3 times with PBS buffer (pH 7.4) and pulverized by a mortar and pestle in liquid nitrogen. The powdered tissue was homogenized with glass tissue blender in ten volumes of PBS buffer (pH 7.4) on ice. After centrifuged at 3500 × *g* for 10 min at 4 °C, the supernatant was pelleted at 35,000 × *g* for 30 min at 4 °C. The virus pellet was resuspended with TMP buffer (100 mM Tris–HCl, pH 7.5, 10 mM $MgCl_2$, 1 mM PMSF) incubated with DNase I and RNase A at 37 °C for 15 min. Then the virus was layered on 20–50% (w/w) sucrose gradient and further purified by centrifugation for 2 h at 60,000×*g* in an SW41 Ti rotor (Beckman). Viral DNA was extracted by incubating virions in 0.5 mg/ml proteinase K and 0.5% SDS at 55 °C for 3 h. After extractions with phenol-chloroform, the DNA was precipitated with ethanol (Sambrook et al., 1989).

PCR amplification and sequencingx

The complete genomic DNA of OSGIV was sequenced by PCR method. As OSGIV showed high homology to ISKNV, the primers were derived from the DNA sequence of ISKNV in GenBank/EMBL/DDBJ database (AF371960). Amplified PCR products were about 1000–1200 bp in length, and primer pairs with overlapping sequence were designed and used in order to fill gaps and verify the sequence. The PCR products were purified using QIAquick PCR purification kit (QIAGEN). DNA sequencing was carried out using BigDye Terminator Kit (Applied Biosystems, Inc.) on an ABI PRISM 377 DNA sequencer (Applied Biosystems, Inc.). The software Data Collection and Sequence Analysis (Applied Biosystems, Inc.) was applied to create the contigs assemble the genome.

Computer-assisted analyses

Genomic DNA composition, structure, and homologous regions were analyzed using DNASTAR (Lasergene). The ORFs and their amino acid sequences were predicted using DS GENE 1.5 (Accelrys Inc.) and NCBI ORF finder (http://www.ncbi.nlm.nih.gov/gorf/gorf.html). Protein database searches were conducted using the BLASTP at NCBI Web site (http://www.ncbi.nlm.nih.gov/). Alignment of amino acid sequences of the major capsid protein, ATPase, cytosine DNA methyl transferase, and DNA polymerase were obtained by Clustal-X 1.80 (Thompson et al., 1994). The phylogenetic trees were generated using the PHYLIP package (Felsenstein, 1995) and the TreeView (Page, 1996). The DNA dot matrix was obtained using DS GENE 1.5 (Accelrys Inc.). Prediction of transmembrane domains (TMs) was performed using TMHMM 2.0 (http://www.cbs.dtu.dk/services/TMHMM-2.0/) (Krogh et al., 2001).

Virus abbreviations

The names of viruses were abbreviated in this article as follow: ALIV, African lampeye iridovirus; ATV, *A. tigrinum* virus; BIV, Bohle iridovirus; CIV, *Chilo* iridescent virus; CzIV, *Costelytra zealandica* iridescent virus; DGIV, dwarf gourami iridovirus; EHNV, epizootic hemorrhagic disease virus; FV3, frog virus 3; GIV, grouper iridovirus; GSDIV, grouper sleepy disease iridovirus; GSIV, giant seaperch iridovirus; ISKNV, infectious spleen and kidney necrosis virus; LBIV, largemouth bass iridovirus; LCDV-1, lymphocystis disease virus 1; LCDV-C, lymphocystis disease virus isolated in China; LYCIV, large yellow croaker iridovirus; OSGIV, orange-spotted grouper iridovirus PBCV-1, *Paramecium bursaria* Chlorella virus 1; RBIV, rock bream iridovirus; RRV, Regina ranavirus; RSIV, red sea bream iridovirus; SBIV, sea bass iridovirus; SGIV, Singapore grouper iridovirus; SIV, *Simulium* iridescent virus; TFV, tiger frog virus; TGIV, grouper iridovirus in Taiwan; TIV, *Tipula* iridescent virus; and WIV, *Wiseana* iridescent virus.

Nucleotide sequence accession number

The nucleotide sequence reported in this paper will appear in the GenBank/EMBL/DDBJ database with the accession number AY894343.

Acknowledgments

This study was supported by grants from the National Science Foundation of China (30271030, 30325035), National “863” project of China (2001AA626030), and Natural Science Foundation of Guangdong Province of China (200230002).

References

Arnér, E.S.J., Eriksson, S., 1995. Mammalian deoxyribonucleoside kinases. Pharmacol. Ther. 67, 155–186.

Bieganowski, P., Garrison, P.N., Hodawadekar, S.C., Faye, G., Barnes, L.D., Brenner, C., 2002. Adenosine monophosphoramidase activity of Hint and Hnt1 supports function of Kin28, Ccl1, and Tfb3. J. Biol. Chem. 277, 10852–10860.

Brader, S., Eccles, SA., 2004. Phosphoinositide 3-kinase signalling pathways in tumor progression, invasion and angiogenesis. Tumori 90, 2–8.

Brenner, C., 2002. Hint, Fhit, and Galt: function, structure, evolution, and mechanism of three branches of the histidine triad superfamily of nucleotide hydrolases and transferases. Biochemistry 41, 9003–9014.

Chen, X.H., Lin, K.B., Wang, X.W., 2003. Outbreaks of an iridovirus disease in maricultured large yellow croaker, *Larimichthys crocea* (Richardson), in China. J. Fish Dis. 26, 615–619.

Chou, H.Y., Hsu, C.C., Peng, T.Y., 1998. Isolation and characterization of a pathogenic iridovirus from cultured grouper (*Epinephelus* sp.) in Taiwan. Fish Pathol. 33, 201–206.

Chua, H.C., Ng, M.L., Woo, J.J., Wee, J.Y., 1994. Investigation of outbreaks of a novel disease, 'Sleepy Grouper Disease', affecting the brown-spotted grouper, *Epinephelus tauvina* Forskal. J. Fish Dis. 17, 417–427.

Danayadol, Y., Direkbusarakom, S., Boonyaratpalin, S., Miyazaki, T., Miyata, M., 1996. An outbreak of iridovirus-like infection in brown-spotted grouper (*Epinephelus malabaracus*) cultured in Thailand. AAHRI Newslett. 5, 6.

Darai, G., Anders, K., Koch, H.G., Delius, H., Gelderblom, H., Samalecos, C., Flugel, R.M., 1983. Analysis of the genome of fish lymphocystis disease virus isolated directly from epidermal tumours of pleuronectes. Virology 126, 466–479.

Darai, G., Delius, H., Clarke, J., Apfel, H., Schnitzler, P., Flugel, R.M., 1985. Molecular cloning and physical mapping of the genome of fish lymphocystis disease virus. Virology 146, 292–301.

Delius, H., Darai, G., Flugel, R.M., 1984. DNA analysis of insect iridescent virus 6: evidence for circular permutation and terminal redundancy. J. Virol. 49, 609–614.

Deng, M., He, J.G., Weng, S.P., Zeng, K., Zeng, Z., Long, Q.X., 2001. Purification and genomic analysis of infectious spleen and kidney necrosis virus (ISKNV) from mandarinfish. J. fisheries of China (Abstract in English) 25, 238–243.

Do, J.W., Moon, C.H., Kim, H.J., Ko, M.S., Kim, S.B., Son, J.H., Kim, J.S., An, E.J., Kim, M.K., Lee, S.K., Han, M.S., Cha, S.J., Park, M.S., Park, M.A., Kim, Y.C., Kim, J.W., Park, J.W., 2004. Complete genomic DNA sequence of rock bream iridovirus. Virology 325, 351–363.

Eaton, B.T., Hyatt, A.D., Hengstberger, S., 1991. Epizootic haematopoietic necrosis virus: purification and classification. J. Fish Dis. 14, 157–169.

Essani, K., 1990. The DNA methylase of frog virus 3. In: Darai, G. (Ed.), Molecular Biology of Iridoviruses. Kluwer, Boston, pp. 163–172.

Evans, E., Klemperer, N., Ghosh, R., Traktman, P., 1995. The vaccinia virus D5 protein, which is required for DNA replication, is a nucleic acid-independent nucleoside triphosphatase. J. Virol. 69, 5253–5361.

Felsenstein, J., 1995. PHYLIP (Phylogeny Inference Package) Version 3.6. University of Washington.

Gelinas, D.S., Bernatchez, P.N., Rollin, S., Bazan, N.G., Sirois, M.G., 2002. Immediate and delayed VEGF-mediated NO synthesis in endothelial cells: role of PI3K, PKC and PLC pathways. Br. J. Pharmacol. 137, 1021–1030.

Goorha, R., Murti, K.G., 1982. The genome of frog virus 3, an animal DNA virus, is circularly permuted and terminally redundant. Proc. Natl. Acad. Sci. U.S.A. 79, 248–252.

He, J.G., Wang, S.P., Zeng, K., Huang, Z.J., Chan, S.M., 2000. Systemic disease caused by an iridovirus-like agent in cultured mandarin fish, *Siniperca chuatsi* (Basilewsky), in China. J. Fish Dis. 23, 219–222.

He, J.G., Deng, M., Weng, S.P., Li, Z., Zhou, S.Y., Long, Q.X., Wang, X.Z., Chan, S.M., 2001. Complete genome analysis of the mandarin fish infectious spleen and kidney necrosis iridovirus. Virology 291, 126–139.

He, J.G., Lü, L., Deng, M., He, H.H., Weng, S.P., Wang, X.H., Zhou, S.Y., Long, Q.X., Wang, X.Z., Chan, S.M., 2002. Sequence analysis of the complete genome of an iridovirus isolated from the tiger frog. Virology 292, 185–197.

Hyatt, A.D., Gould, A.R., Zupanovic, Z., Cunningham, A.A., Hengstberger, S., Whittington, R.J., Kattenbelt, J., Coupar, B.E.H., 2000. Comparative studies of piscine and amphibian iridoviruses. Arch. Virol. 145, 301–331.

Inouye, K., Yamano, K., Maeno, Y., Nakajima, K., Matsuoka, M., Wada, Y., Sorimachi, M., 1992. Iridovirus infection of cultured red sea bream, *Pagrus major*. Fish Pathol. 27, 19–27.

Jakob, N.J., Muller, K., Bahr, U., Darai, G., 2001. Analysis of the first complete DNA sequence of an invertebrate iridovirus: coding strategy of the genome of Chilo iridescent virus. Virology 286, 182–196.

Jancovich, J.K., Mao, J.H., Chinchar, V.G., Wyatt, C., Case, S.T., Kumar, S., Valente, G., Subramanian, S., Davidson, E.W., Collins, J.P., Jacobs, B.L., 2003. Genomic sequence of a ranavirus (family Iridoviridae) associated with salamander mortalities in North America. Virology 316, 90–103.

Jung, S.J., Oh, M.J., 2000. Iridovirus-like infection associated with high mortalities of striped beakperch, *Oplegnathus fasciatus* (Temmink et Schlegel), in southern coastal areas of the Korean peninsula. J. Fish Dis. 23, 223–226.

Krogh, A., Larsson, B., von Heijne, G., Sonnhammer, E.L., 2001. Predicting transmembrane protein topology with a hidden Markov model: application to complete genomes. J. Mol. Biol. 305, 567–580.

Lammers, M., Follmann, H., 1983. The ribonucleotide reductases—a unique group of metalloenzymes essential for cell proliferation. Struct. Bonding 54, 27–91.

Lü, L., He, J.G., He, H.H., Deng, M., Wang, X.H., Weng, S.P., 2001. Purification and enzyme analysis of a virus from Frog (*Rana tigrina rugulosa*). Acta Scientiarum Naturalium Universitatis Sunyatseni (Abstract in English) 40, 91–95.

Lu, L., Holmqvist, K., Cross, M., Welsh, M., 2002. Role of the Src homology 2 domain-containing protein Shb in murine brain endothelial cell proliferation and differentiation. Cell Growth Differ. 13, 141–148.

McGrogan, D.G., Ostland, V.E., Byrne, P.J., Ferguson, H.W., 1998. Systemic disease involving an iridovirus-like agent in cultured tilapia, *Oreochromis niloticus* L. J. Fish Dis. 21, 149–152.

Nakajima, K., Sorimachi, M., 1995. Production of monoclonal antibodies against red sea bream iridovirus. Fish Pathol. 30, 47–52.

Page, R.D., 1996. Tree View: an application to display phylogenetic trees on personal computers. Comput. Appl. Biosci. 12, 357–358.

Rauh, M.J., Kalesnikoff, J., Hughes, M., Sly, L., Lam, V., Krystal, G., 2003. Role of Src homology 2-containing-inositol 5′-phosphatase (SHIP) in mast cells and macrophages. Biochem. Soc. Transact. 31, 286–291.

Rodge, H.D., Kobs, M., Macartney, A., Frerichs, G.N., 1997. Systemic iridovirus infection in freshwater angelfish, *Pterophyllum scalare* (Lichtenstein). J. Fish Dis. 20, 69–72.

Sambrook, J., Fritsch, E.F., Maniatis, T., 1989. Extraction, purification, and analysis of message RNA from eukaryotic cells. Molecular cloning: A Laboratory Manual. Cold Spring Harbor Laboratory Press, Plainview, New York.

Saitou, N., Nei, M., 1987. The neighbor-joining method: a new method for reconstructing phylogenetic trees. Mol. Biol. Evol. 4, 406–425.

Senkevich, T.G., Koonin, E.V., Bugert, J.J., Darai, G., Moss, B., 1997. The genome of molluscum contagiosum virus: analysis and comparison with other poxviruses. Virology 233, 19–42.

Senkevich, T.G., White, C.L., Koonin, E.V., Moss, B., 2000. A viral member of the ERV1/ALR protein family participates in a cytoplasmic pathway of disulfide bond formation. Proc. Natl. Acad. Sci. U.S.A. 97, 12068–12073.

Shi, C.Y., Wang, Y.G., Yang, S.L., Huang, J., Wang, Q.Y., 2004. The first report of an ridovirus-like gent infection in farmed turbot, *Scophthalmus maximus*, in China. Aquaculture 236, 11–25.

Shim, E.K., Moon, C.S., Lee, G.Y., Ha, Y.J., Chae, S.K., Lee, J.R., 2004. Association of the Src homology 2 domain-containing leukocyte phosphoprotein of 76 kD (SLP-76) with the p85 subunit of phosphoinositide 3-kinase. FEBS Lett. 575, 35–40.

Song, W.J., Qin, Q.W., Qiu, J., Huang, C.H., Wang, F., Hew, C.L., 2004. Functional genomics analysis of Singapore grouper iridovirus: complete sequence determination and proteomic analysis. J. Virol. 78, 12576–12590.

Sudthongkong, C., Miyata, M., Miyazaki, T., 2001. Iridovirus disease in two ornamental tropical freshwater fishes: African lampeye and dwarf gourami. Dis. Aquat. Org. 48, 163–173.

Sudthongkong, C., Miyata, M., Miyazaki, T., 2002. Viral DNA sequence of genes encoding the ATPase and the major capsid protein of tropical iridovirus isolates which are pathogenic to fishes in Japan, South China Sea and Southeast Asian countries. Arch. Virol. 147, 2089–2109.

Takahashi, M., Matsui, A., Inao, M., Mochida, S., Fujiwara, K., 2003. ERK/MAPK-dependent PI3K/Akt phosphorylation through VEGFR-1 after VEGF stimulation in activated hepatic stellate cells. Hepatol. Res. 26, 232–236.

Tan, W.G.H., Barkman, T.J., Chinchar, V.G., Essani, K., 2004. Comparative genomic analyses of frog virus 3, type species of the genus *Ranavirus* (family Iridoviridae). Virology 323, 70–84.

Thompson, J.D., Higgins, D.G., Gibson, T.J., 1994. CLUSTALW: improving the sensitivity of progressive multiple sequence alignment through sequence weighting, position-specific gap penalties and weight matrix choice. Nucleic Acids Res. 22, 4673–4680.

Tidona, C.A., Darai, G., 1997. The complete DNA sequence of lymphocystis disease virus. Virology 230, 207–216.

Tidona, C.A., Schnitzler, P., Kehm, R., Darai, G., 1998. Is the major capsid protein of iridoviruses a suitable target for the study of viral evolution? Virus Genes 16, 59–66.

van Hulten, M.C.W., Witteveldt, J., Peters, S., Kloosterboer, N., Tarchini, R., Fiers, M., Sandbrink, H., Lankhorst, R., Vlak, K., 2001. The white spot syndrome virus DNA genome sequence. Virology 286, 7–22.

van Regenmortel, M.H., Fauquet, C.M., Bishop, D.H.L., Carstens, E.B., Estes, M.K., Lemon, S.M., Maniloff, J., Mayo, M.A., McGeoch, D.J., Pringle, C.R., Wickner, R.B., 1999. Virus Taxonomy-Seventh Report of the International Committee on Taxonomy of Viruses. Academic Press, New York.

Weng, S.P., Wang, Y.Q., He, J.G., Deng, M., Lü, L., Guan, H., Liu, .J., Chan, Y.J., 2002. Outbreaks of an iridovirus in red drum, *Sciaenops ocellata* (L.), cultured in southern China. J. Fish Dis. 25, 681–685.

Williams, T., 1996. The iridoviruses. Adv. Virus Res. 46, 345–412.

Willis, D.B., Granoff, A., 1980. Frog virus 3 DNA is heavily methylated at CpG sequences. Virology 107, 250–257.

Willis, D., Foglesong, D., Granoff, A., 1984. Nucleotide sequence of an immediate-early frog virus 3 gene. J. Virol. 53, 905–912.

Wanger, H., Simon, D., Werner, E., Gelderblom, H., Darai, G., 1985. Methylation pattern of DNA of fish lymphocystis disease virus. J. Virol. 53, 1005–1007.

Zhang, Q.Y., Xiao, F., Xie, J., Li, Z.Q., Gui, J.F., 2004. Complete genome sequence of lymphocystis disease virus isolated from China. J. Virol. 78, 6982–6994.